Biomedicine & Pharmacotherapy 181 (2024) 117709

Contents lists available at ScienceDirect

Biomedicine & Pharmacotherapy

journal homepage: www.elsevier.com/locate/biopha

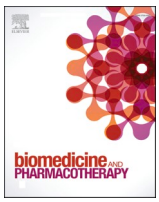

# Febuxostat enhances the efficacy of dasatinib by inhibiting ATP-binding cassette subfamily G member 2 (ABCG2) in chronic myeloid leukemia cells

Kotaro Kawashima [a,1], Kenji Ikemura [b,c,*,1], Miho Takemura [d], Yuji Toyozumi [a], Masahiro Okuda [b,c]

[a] Department of Hospital Pharmacy, School of Pharmaceutical Sciences, Osaka University, Suita, Osaka 5650871, Japan
[b] Department of Pharmacy, Osaka University Hospital, Suita, Osaka 5650871, Japan
[c] Department of Hospital Pharmacy, Graduate School of Medicine, Osaka University, Suita, Osaka 5650871, Japan
[d] Department of Clinical Pharmacy Research and Education, Graduate School of Pharmaceutical Sciences, Osaka University, Suita, Osaka 5650871, Japan

ARTICLE INFO

*Keywords:*
ATP-binding cassette subfamily G member 2
Chronic myeloid leukemia
Dasatinib
Febuxostat

ABSTRACT

Dasatinib is a second-generation breakpoint cluster region-abelson 1 (BCR::ABL1) tyrosine kinase inhibitor (TKI) used for the treatment of chronic myeloid leukemia (CML). Overexpression of ATP-binding cassette subfamily G member 2 (ABCG2) in CML cells contributes to dasatinib resistance and poor chemotherapeutic responses. Considering that the xanthine oxidase inhibitor febuxostat has anti-ABCG2 activity, febuxostat may enhance the efficacy of dasatinib. However, the mechanism of action of febuxostat and its effects on the efficacy and safety of dasatinib in patients with CML are unknown. Therefore, this study aimed to retrospectively investigate the clinical impact of concomitant febuxostat on the efficacy of dasatinib in 65 patients with CML. Moreover, its underlying mechanism was explored *in vitro* using an ABCG2-overexpressing CML cell line (K562-ABCG2 cells). The retrospective study revealed that the achievement ratios of early molecular response at three months and major molecular response at 12 months after dasatinib treatment in patients with febuxostat were significantly higher than those in patients without febuxostat (91 % vs. 70 %, $p = 0.034$, 86 % vs. 53 %, $p = 0.013$, respectively). *In vitro* studies showed that febuxostat significantly decreased cell viability and increased the residual dasatinib concentration in dasatinib-treated K562-ABCG2 cells. Moreover, phosphorylated BCR::ABL1 levels in dasatinib-treated K562-ABCG2 cells were significantly decreased by febuxostat. Overall, concomitant febuxostat enhanced the efficacy of dasatinib in patients with CML. This was achieved partially by inhibition of ABCG2-mediated excretion of dasatinib from CML cells. Therefore, these findings provide important insights for improving CML treatment and overcoming TKI resistance.

## 1. Introduction

Chronic myeloid leukemia (CML) is a clonal myeloproliferative malignancy. The disease is characterized by abnormal and persistent breakpoint cluster region-abelson 1 (BCR::ABL1) tyrosine kinase activity due to the reciprocal translocation between chromosomes 9 and 22 [1]. Dasatinib is a second-generation BCR::ABL1 tyrosine kinase inhibitor (TKI) that has emerged as a primary CML treatment for patients with imatinib-resistance or intolerance [2]. The advent of dasatinib has largely improved the prognosis for patients with CML [2]; however, treatment failure due to acquired resistance to second-generation TKIs, including dasatinib, has emerged as a significant concern [3]. Thus, therapeutic strategies are needed to overcome TKI-resistance in CML treatment.

BCR::ABL1-dependent and -independent mechanisms contribute to TKI resistance [4]. BCR::ABL1-dependent pathways involve BCR::ABL1 mutations, gene amplification, or upregulated expression. In contrast, BCR::ABL1-independent resistance is associated with altered expression and/or function of influx and efflux transporters in CML cells [4]. In particular, ATP-binding cassette subfamily G member 2 (ABCG2), plays a crucial role in the extrusion of endogenous and exogenous substrates including anticancer agents [5]. Overexpression of ABCG2 in CML cells results in increased TKI efflux from CML cells, thereby contributing to TKI resistance and a poor chemotherapeutic response [6,7]. Moreover, a

* Correspondence to: Department of Pharmacy, Osaka University Hospital, 2-15 Yamadaoka, Suita, Osaka 565-0871, Japan.
*E-mail address:* ikemurak@hp-drug.med.osaka-u.ac.jp (K. Ikemura).
[1] Kotaro Kawashima and Kenji Ikemura contributed equally to this work

https://doi.org/10.1016/j.biopha.2024.117709
Received 24 September 2024; Received in revised form 20 November 2024; Accepted 22 November 2024
Available online 25 November 2024

single-nucleotide polymorphism in *ABCG2*, which adversely affects the function of ABCG2, enhanced clinical outcomes in patients with CML receiving imatinib [8]. Therefore, the strategy of inhibiting the activity and/or function of ABCG2 may elevate intracellular TKI concentrations in CML cells and enhance the efficacy of TKIs in patients with CML.

Febuxostat is a non-purine selective xanthine oxidase inhibitor that effectively prevents hyperuricemia accompanied by tumor lysis syndrome during cancer chemotherapy with TKIs [9]. Febuxostat potently inhibited ABCG2-mediated transport of ABCG2 substrates at clinical concentrations [10,11]. Moreover, febuxostat increased the intracellular concentration of nilotinib, which is a TKI, and enhanced nilotinib efficacy in an imatinib-resistant CML cell line (K562 cells) [12]. However, the effects of febuxostat on ABCG2 inhibition and on the efficacy and safety of TKIs in patients with CML remains to be elucidated.

Therefore, this retrospective study aimed to evaluate the clinical impact of concomitant febuxostat on the efficacy and safety of dasatinib in patients with CML using electronic medical records. In addition, the underlying mechanism was explored *in vitro* using a human CML cell line (K562 cells).

## 2. Materials and methods

### 2.1. Materials

Allopurinol and imatinib were sourced from FUJIFILM Wako Chemicals (Osaka, Japan). Dasatinib was obtained from Toronto Research Chemicals (North York, Ontario, Canada). Febuxostat was acquired from Tokyo Chemical Industry (Tokyo, Japan). Fumitremorgin C (FTC) was purchased from Adipogen Life Sciences (San Diego, CA). All other chemicals used were of the highest purity available.

### 2.2. Retrospective study in patients receiving dasatinib

Clinical data were extracted from electronic medical records of 90 hospitalized patients who received dasatinib (SPRYCEL® Tables, Bristol-Myers Squibb) to treat chronic-phase CML at Osaka University Hospital from January 2009 to April 2022. Patients were excluded if they had missing data. In addition to the use of febuxostat, periodic co-administration drugs that may cause potential interactions were identified by Lexicomp® Lexi-Interact™ Online (Lexi-Comp, Inc., Hudson, OH). The dosage of febuxostat during dasatinib therapy was adjusted according to the package insert. Early molecular response (EMR) was defined as BCR::ABL1$^{IS} \leq 10$ % at three months after dasatinib treatment. Major molecular response (MMR) was defined as BCR::ABL1$^{IS} \leq$ 0.1 % at 12 months after dasatinib treatment. Adverse events leading to discontinuation of dasatinib therapy were evaluated according to the Common Terminology Criteria for Adverse Events version 4.0. Time to treatment failure (TTF) of dasatinib therapy was defined as the time from the initiation of dasatinib therapy to treatment discontinuation. This study was conducted in accordance with the Declaration of Helsinki and approved by the ethical review board of Osaka University Hospital (No. 16002–11). Informed consent was obtained via opt-out through the website.

### 2.3. Cell culture

Human CML cells (K562 cells) ware obtained from the Japanese Collection of Research Bioresources Cell Bank (Osaka, Japan), and cultured in RPMI-1640 supplemented with 10 % fetal bovine serum. K562 cells were used between passage numbers 21 and 48. The cells were maintained at 37°C under 5 % $CO_2$ in a humidified atmosphere.

### 2.4. Establishment of stable human ABCG2-expressing K562 cells

K562 cells were seeded onto 24-well plates at a density of $4.0 \times 10^5$ cells per well. The cells were transfected with 0.5 μg of pRP[Exp]-Neo-CAG>hABCG2 plasmid vector [NM_001348985.1] (VectorBuilder, Chicago, IL) per well using Lipofectamin® 3000 (Invitrogen, Carlsbad, CA) according to the manufacturer's instructions. After 48 h of transfection, the cells that were split at a ratio of 1:10 were cultured in culture medium containing G418 (0.5 mg/mL). Single colonies were then selected and subsequently grown. Membrane proteins of the cells were extracted using the Mem-PER™ Plus Membrane Protein Extraction Kit (ThermoFisher Scientific, Waltham, MA) according to the manufacturer's instructions. The expressions of human ABCG2 and $Na^+/K^+$-ATPase (a plasma membrane marker) in wild-type K562 (K562-WT) and ABCG2-expressing K562 cells (K562-ABCG2) cells were confirmed using western blotting analysis.

### 2.5. Viability of K562-WT and K562-ABCG2 cells

K562-WT and K562-ABCG2 cells were seeded on a 96 well-plate at a density of $5 \times 10^3$ cells/well. To calculate the 50 % inhibitory concentration ($IC_{50}$) values of imatinib and dasatinib, the cells were incubated at 37°C for 72 h with culture medium containing various imatinib and dasatinib concentrations. To evaluate the effects of febuxostat on the efficacy of dasatinib, the cells were incubated with vehicle (control) or dasatinib (1.5 nM) in the absence or presence of febuxostat (1, 5, and 10 μM), FTC (typical ABCG2 inhibitor, 5 μM), and allopurinol (xanthine oxidase inhibitor, negative control, 10 μM) at 37°C for 72 h. After incubation, the cell viability was determined using the Cell Counting Kit-8 (Dojindo Laboratories, Kumamoto, Japan) according to the manufacturer's instructions. The absorbance was measured at 450 nm using the Multiskan™ FC Microplate Absorbance Reader (ThermoFisher Scientific). The cell viability after treatment with the vehicle (control) was set at 100 %. The $IC_{50}$ values were generated from curves using GraphPad Prism version 8.4.3 (GraphPad Software Inc., San Diego, CA). To identify the nature of interaction between dasatinib and febuxostat, the combination index values were calculated using SynergyFinder web application according to the method by Chou and Talalay [13].

### 2.6. Effect of febuxostat on dasatinib concentrations in K562-WT and K562-ABCG2 cells

K562-WT and K562-ABCG2 cells ($5.0 \times 10^5$ cells) were incubated with 1 mL of incubation medium containing 10 μM dasatinib at 37°C for 30 min. The composition of the incubation medium was as follows: 145 mM NaCl, 3 mM KCl, 1 mM $CaCl_2$, 0.5 mM $MgCl_2$, 5 mM D-glucose, and 5 mM HEPES (pH 7.4). After dasatinib was removed by rinsing three times with ice-cold phosphate buffer saline (PBS), the cells were incubated with febuxostat (10 μM), FTC (a typical ABCG2 inhibitor, 5 μM), or allopurinol (negative control, 10 μM) at 37°C for 30 min. Subsequently, the cells were incubated with incubation medium in the presence of 4 mM ATP. After 5 min, the cells were rinsed once with ice-cold PBS containing 1 % bovine serum albumin and twice with ice-cold PBS. To evaluate residual concentration of dasatinib in cells, dasatinib was extracted using 300 μL of 50 % methanol. The concentration of dasatinib was determined using liquid chromatography with tandem mass spectrometry (LC-MS/MS).

### 2.7. Dasatinib concentration in K562-WT and K562-ABCG2 cells

LC-MS/MS was employed to determine the dasatinib concentrations in K562-WT and K562-ABCG2 cells using a previously described method [14]. The LC-MS/MS system was applied with the ACQUITY HPLC H-class/ACQUITY TQD with electrospray ionization (Waters, Milford, MA). First, 5 μL of 1 μM imatinib, utilized as an internal standard (IS), was added to the samples (50 μL). The samples (10 μL) were then subjected to LC-MS/MS. LC separations were performed on an InterSustainSwift C18 HP column (2.1 × 150 mm, 3 μm, GL Sciences, Tokyo, Japan) maintained at 40°C with a flow rate of 0.2 mL/min. Solvent A was water with 0.1 % formic acid, and solvent B was acetonitrile with

0.1 % formic acid. The entire LC gradient was 17 min. Mobile phase B was initially at 15 %, was increased to 95 % from 1–10 min, and then decreased back to 15 % from 12–17 min. Dasatinib and IS were detected in multiple reaction monitoring mode. MS/MS conditions involved cone voltages and collision energies of 70 V/60 eV (dasatinib) and 50 V/30 eV (IS) in positive mode, respectively. MS/MS monitoring ions were as follows: dasatinib (*m/z* 488.36 $[M + H]^+ \rightarrow$ *m/z* 232.45) and IS (*m/z* 494.49 $[M + H]^+ \rightarrow$ *m/z* 394.42). The desolvation temperature was 350°C, cone gas flow was 50 L/h, and desolvation gas flow was 600 L/h. All LC-MS/MS data were collected and processed using Masslynx 4.1 software (Waters, Milford, MA).

### 2.8. Evaluation of dasatinib-mediated BCR::ABL1 dephosphorylation

To assess the BCR::ABL1 dephosphorylation efficacy of dasatinib, K562-WT and K562-ABCG2 cells were seeded on a 60-mm dish at a density of $2.5 \times 10^5$ cells/well. The cells were incubated with culture medium containing 1.5 nM dasatinib in the absence or presence of febuxostat (10 μM) or FTC (5 μM). After 72 h, total soluble protein lysates were extracted using RIPA Lysis and Extraction Buffer (ThermoFisher Scientific) according to the manufacturer's instructions. The expression of phosphorylated BCR::ABL1 (p-BCR::ABL1), BCR::ABL1, and β-actin in each cell were determined using western blotting analyses.

### 2.9. Western blotting analyses

The membrane fraction (1 μg) or total protein (10 μg) of K562-WT and K562-ABCG2 cells were separated using NuPAGE Novex 4 –12 % Bis-Tris Gel (Invitrogen) and were then transferred onto polyvinylidene fluoride membranes (Invitrogen). Western blotting was performed using anti-ABCG2 antibody (BXP-21, Santa Cruz Biotechnology, Dallas, TX), anti-ATP1A1 antibody (14418–1-AP, Proteintech, Rosemont, IL) for $Na^+/K^+$-ATPase, phospho-BCR (Tyr177) antibody (#3901, Cell Signaling Technology, Danvers, MA) for p-BCR::ABL1, c-Abl (8E9) antibody (sc-56887, Santa Cruz Biotechnology, Dallas, TX) for BCR::ABL1, and β-actin (13E5) antibody (#4970, Cell Signaling Technology, Danvers, MA) for β-actin according to the manufacturer's instructions. The relative densities of the bands in each lane were determined using Image Lab 6.1 (Bio-Rad Laboratories, Hercules, CA), and the densitometric ratios of ABCG2 to $Na^+/K^+$-ATPase as well as those of p-BCR::ABL1 and BCR::ABL1 to β-actin were calculated.

### 2.10. Statistical analyses

The results of the *in vitro* experimental data are expressed as the mean ± standard error (S.E.). Statistical analyses for multiple groups were carried out using one-way analysis of variance followed by Dunnett's test or Tukey's multiple comparison test. Differences between two groups in the *in vitro* study were determined using the unpaired t-test. For the clinical study, statistical comparisons between the two groups were performed using the Mann-Whitney U-test and Fisher's exact test for continuous and categorical variables, respectively. TTF was analyzed using the Kaplan–Meier curve method and log-rank test. All statistical analyses were performed using GraphPad Prism 8.43 (GraphPad Software Inc., San Diego, CA). Differences were considered significant at $p < 0.05$.

## 3. Results

### 3.1. Patient characteristics

According to the inclusion and exclusion criteria, 65 of the 90 patients were enrolled in this study. The characteristics of patients with and without febuxostat are summarized in Table 1. Twenty-two patients (34 %) received febuxostat, whereas 43 patients (66 %) did not receive febuxostat. Overall, 8 patients (15 %) were treated with imatinib, and 3 patients (5 %) received nilotinib prior to initiating dasatinib therapy. No significant differences were observed between patients treated with and without febuxostat in terms of patient characteristics. The median dose and duration [range] of febuxostat treatment after dasatinib therapy were 20 [10−60] mg and 30 [5−365] days, respectively.

**Table 1**
Patient characteristics.

| | Without febuxostat (n = 43) | With febuxostat (n = 22) | *p* value |
|---|---|---|---|
| Age (years) | 56 [24–86] | 55 [22–77] | 0.750 |
| Male | 25 (58) | 15 (68) | 0.304 |
| Body weight (kg) | 64.5 [44.0–113.7] | 59.8 [43.3–124.0] | 0.723 |
| Initial dasatinib dose (mg) | 100 [40–140] | 100 [40–140] | 0.108 |
| Baseline biological parameters | | | |
| AST (U/L) | 24 [9–45] | 26 [10–55] | 0.722 |
| ALT (U/L) | 23 [5–53] | 22 [10–81] | 0.763 |
| Scr (mg/dL) | 0.80 [0.54–1.23] | 0.75 [0.51–1.51] | 0.579 |
| BUN (mg/dL) | 14 [9–21] | 16 [10–26] | 0.539 |
| WBC ($\times 10^9$/L) | 9.36 [1.59–76.83] | 16.01 [0.21–89.84] | 0.122 |
| PLT ($\times 10^9$/L) | 265 [67–1551] | 158 [21–1197] | 0.194 |
| ANC ($\times 10^9$/L) | 6.21 [0.58–63.69] | 9.14 [0.03–47.63] | 0.370 |
| Hb (g/dL) | 12.3 [8.2–16.6] | 11.5 [7.6–15.3] | 0.327 |
| Prior BCR::ABL1 TKI use | | | |
| Imatinib | 6 (14) | 2 (9) | 0.572 |
| Nilotinib | 2 (5) | 1 (5) | 0.985 |
| Co-administrated drugs | | | |
| $H_2$-receptor antagonists | 5 (12) | 3 (14) | 0.816 |
| Proton pump inhibitors | 4 (9) | 3 (14) | 0.594 |

Values are presented as median [range] or number (%). Statistical analyses were performed using Fisher's exact test or Mann–Whitney U test. ALT, alanine aminotransaminase; ANC, absolute neutrophil count; AST, aspartate aminotransaminase; BUN, blood urea nitrogen; Hb, hemoglobin; PLT, platelet; Scr, serum creatinine; TKI, Tyrosine Kinase Inhibitor; WBC, white blood cell; BCR::ABL1 TKI, breakpoint cluster region-abelson 1 tyrosine kinase inhibitor.

### 3.2. Efficacy and adverse events after dasatinib administration in patients with and without febuxostat

Efficacy (EMR achievement after three months and MMR achievement after 12 months of dasatinib therapy) and adverse events leading to discontinuation of dasatinib are shown in Table 2. Ratios of EMR and MMR achievement in patients with febuxostat were significantly higher than those in patients without febuxostat (91 % vs. 70 %, $p = 0.034$, 86 % vs. 53 %, $p = 0.013$, respectively). In addition, we assessed the

**Table 2**
Efficacy and adverse events following dasatinib administration in patients with and without febuxostat.

| | Without febuxostat (n = 43) | With febuxostat (n = 22) | *p* value |
|---|---|---|---|
| Three months after dasatinib treatment | | | |
| EMR achievement | 30 (70) | 20 (91) | 0.034 |
| Unknown | 2 (5) | 1 (5) | 0.985 |
| 12 months after dasatinib treatment | | | |
| MMR achievement | 23 (53) | 19 (86) | 0.013 |
| Reasons for discontinuation of dasatinib | | | |
| Adverse events | 8 (19) | 2 (9) | 0.267 |
| SD or PD | 6 (14) | 0 (0) | 0.074 |
| Adverse events leading to discontinuation of dasatinib | | | |
| Fluid retention | 9 (21) | 1 (5) | 0.083 |
| Bone marrow suppression | 7 (16) | 3 (14) | 0.780 |
| Bleeding | 5 (12) | 1 (5) | 0.351 |
| Infection | 3 (7) | 0 (0) | 0.205 |
| Interstitial lung disease | 1 (2) | 0 (0) | 0.471 |
| Tumor lysis syndrome | 1 (2) | 0 (0) | 0.471 |
| Hepatotoxicity | 0 (0) | 1 (5) | 0.159 |

Values are presented as number (%). Statistical analyses were performed using the Fisher's exact test. EMR, early molecular response; MMR, major molecular response; PD, progressive disease; SD, stable disease.

impact of concomitant febuxostat on the TTF following dasatinib therapy using Kaplan-Meier analysis (Fig. 1). As shown in Fig. 1, the Kaplan-Meier analysis demonstrated that the TTF following dasatinib therapy was significantly longer in patients receiving febuxostat ($p = 0.043$, Log-rank test). At 12 months after dasatinib treatment, the treatment continuation rate of dasatinib in patients without and with febuxostat was 67 % and 90 %, respectively. In contrast, there were no significant differences between patients treated with and without febuxostat in terms of the incidence of adverse events leading to dasatinib discontinuation (Table 2).

### 3.3. Role of ABCG2 overexpression in TKI resistance in CML cells

To investigate the role of ABCG2 overexpression in TKI resistance in CML cells, K562-ABCG2 cells were established from K562 cells. We first confirmed the ABCG2 expression level in K562-WT and K562-ABCG2 cells using western blotting analysis (Fig. 2A). The ABCG2 expression level in K562-ABCG2 cells was markedly higher than that in K562-WT cells (Fig. 2B). We then assessed the efficacy of TKIs (imatinib and dasatinib) in K562-WT and K562-ABCG2 cells (Fig. 2C and D). The $IC_{50}$ values for imatinib and dasatinib in K562-WT and K562-ABCG2 cells are shown in Table 3. The $IC_{50}$ values for imatinib in K562-WT and K562-ABCG2 cells were 152.8 nM and 342.8 nM, respectively, and those for dasatinib were 0.78 nM and 1.74 nM, respectively. Therefore, TKI resistance was confirmed in K562-ABCG2 cells.

### 3.4. Effect of febuxostat on K562-ABCG2 cell viability after dasatinib exposure

Fig. 3 shows the effect of febuxostat, FTC, and allopurinol on K562-ABCG2 cell viability after dasatinib exposure. Cell viability was reduced to approximately 55 % of that of the control (vehicle) by a single treatment with dasatinib (1.5 nM) for 72 h. The cell viability was further reduced by co-incubation of febuxostat with dasatinib in a concentration-dependent manner. A similar effect was observed after co-incubation with FTC (ABCG2 inhibitor) but not allopurinol (negative control). In contrast, a single treatment with febuxostat (10 μM), FTC (5 μM), and allopurinol (10 μM) showed no significant effects on cell viability. The combination index values for dasatinib with febuxostat at concentrations of 1, 5, and 10 μM were 0.79, 0.66, and 0.51, respectively. As shown in Fig. 3B, the effect-combination index plot indicated that the combination of febuxostat exhibited a synergistic effect.

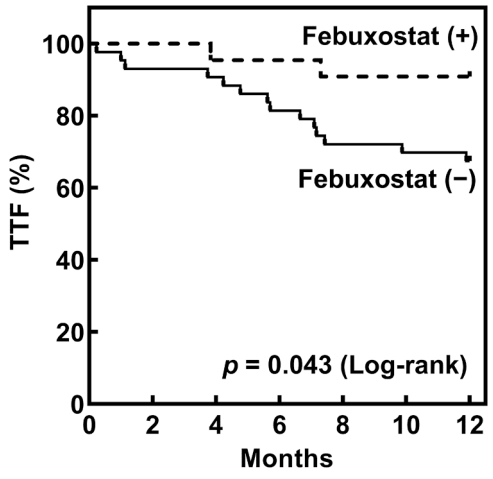


**Fig. 1.** Kaplan–Meier analysis of the time to treatment failure (TTF) following dasatinib treatment in patients with febuxostat (+; n = 22) and without febuxostat (−; n = 43).

### 3.5. Effect of febuxostat on dasatinib concentration in K562-WT and K562-ABCG2 cells

Fig. 4 shows the residual concentration of dasatinib after efflux for 5 min in K562-WT and K562-ABCG2 cells in the absence or presence of 10 μM febuxostat, 5 μM FTC, or 10 μM allopurinol. The residual concentration of dasatinib in K562-ABCG2 cells was significantly lower than that in K562-WT cells. The residual concentration of dasatinib in K562-ABCG2 cells was significantly increased by treatment with febuxostat or FTC. In contrast, allopurinol had no significant effect on the residual concentration of dasatinib in K562-ABCG2 cells.

### 3.6. Effect of febuxostat on p-BCR::ABL1 expression after dasatinib exposure

Fig. 5 shows the western blotting analysis of p-BCR::ABL1, BCR::ABL1, and β-actin expression levels in K562-WT cells (Fig. 5A, B, and C) and K562-ABCG2 cells (Fig. 5D, E, and 5F) after dasatinib exposure in the absence or presence of febuxostat or FTC. The expression of p-BCR::ABL1 and BCR::ABL1 were confirmed in K562-WT and K562-ABCG2 cells. Moreover, exposure to dasatinib significantly inhibited p-BCR::ABL1 expression in K562-WT cells but not in K562-ABCG2 cells (Fig. 5B and E). The p-BCR::ABL1 expression levels in K562-ABCG2 cells after dasatinib exposure were significantly decreased by co-incubation with febuxostat or FTC (Fig. 5E). In contrast, significant changes in the expression of BCR::ABL1 and β-actin were not observed in K562-WT and K562-ABCG2 cells after exposure to each drug.

## 4. Discussion

The clinical impact of febuxostat on the efficacy of dasatinib in patients with CML patients, as well as the antitumor effect of dasatinib through ABCG2 inhibition, remains to be elucidated. To the best of our knowledge, this is the first study reporting the enhanced effect of concomitant febuxostat on the efficacy of dasatinib, at least, in part, by the inhibition of ABCG2-mediated excretion of dasatinib from CML cells.

To clarify the clinical impact of concomitant febuxostat on the efficacy of dasatinib, we conducted a retrospective chart review of patients with CML receiving dasatinib. The study demonstrated that the number of patients with EMRs and MMRs achievement were significantly higher with febuxostat than that without febuxostat (Table 2). In addition, the TTF following dasatinib therapy was significantly longer in patients receiving febuxostat (Fig. 1). Therefore, these findings suggest that concomitant febuxostat enhances the efficacy of dasatinib in patients with CML. In addition, achievement of EMR at three months after dasatinib treatment has been identified as a critical determinant of patient prognosis [15]. Since the median duration of febuxostat treatment after dasatinib therapy were 30 days in our clinical study, it is assumed that the concomitant febuxostat during initial three months of dasatinib therapy is pivotal for ensuring optimal therapeutic outcomes.

Overexpression of ABCG2 on the membrane surface of CML cells contributes to decreased TKI efficacy [6,7]. Thus, we validated the contribution of ABCG2 overexpression to TKI resistance in K562 cells. As shown in Table 3, the $IC_{50}$ values of imatinib and dasatinib in K562-ABCG2 cells were significantly higher than those in K562-WT cells. In addition, the decreased cell viability and residual concentration of dasatinib in K562-ABCG2 cells was restored by co-exposure with FTC (Figs. 3A and 4). Thus, these findings indicated that reduced intracellular dasatinib concentration *via* ABCG2 overexpression contributes to the development of dasatinib resistance, which is consistent with previous reports [6,7].

Subsequently, we investigated the effect of febuxostat on dasatinib efficacy in K562-ABCG2 cells considering that febuxostat potently inhibited ABCG2 activity [10,11]. As shown in Figs. 3A, 4, and 5E, combination with febuxostat increased the efficacy and residual concentrations of dasatinib in K562-ABCG2 cells. In contrast, allopurinol,

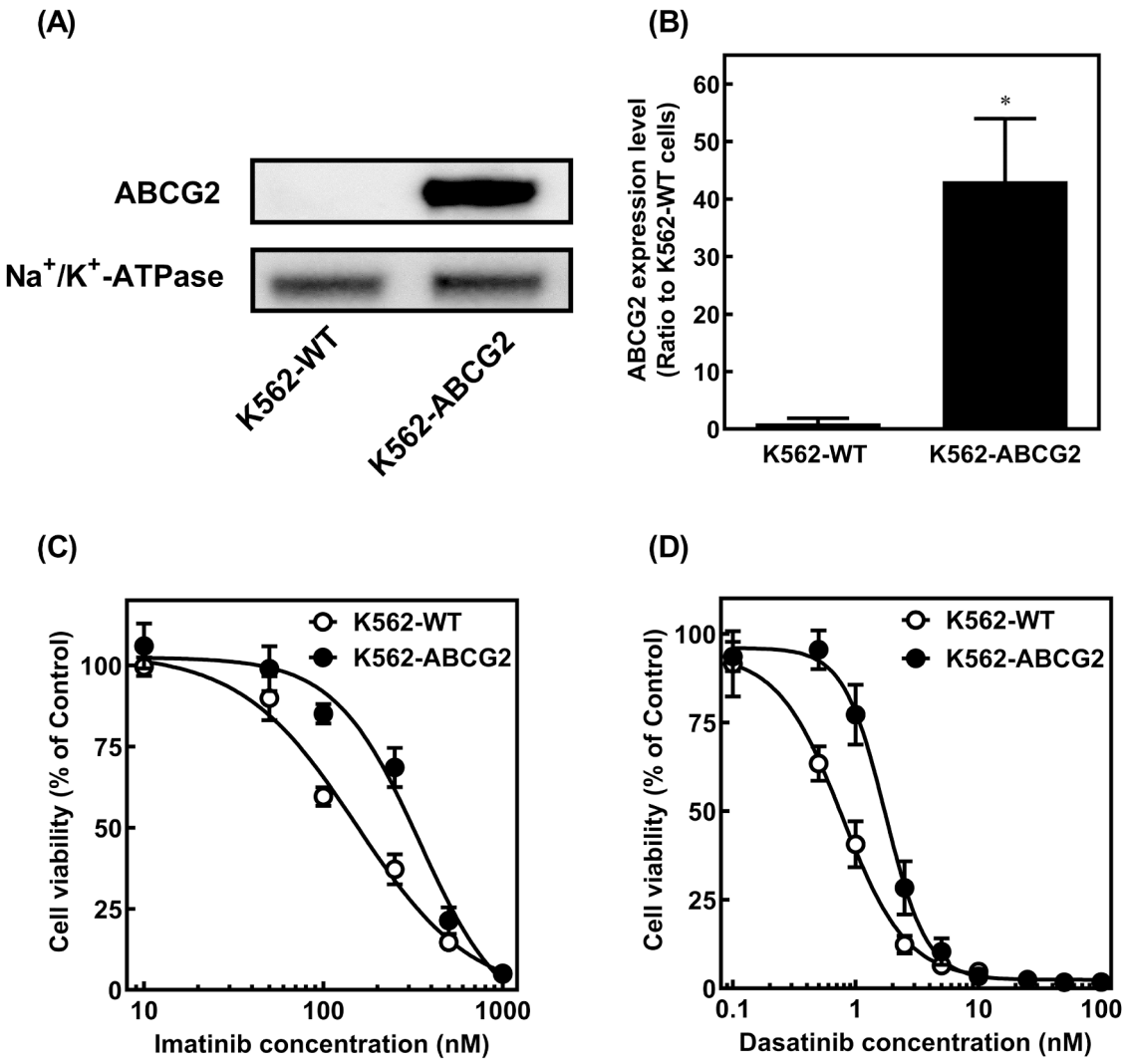


**Fig. 2.** ABCG2 expression and K562-WT and K562-ABCG2 cell viability after imatinib and dasatinib treatment. (A) Western blotting analysis of ABCG2 and $Na^+/K^+$-ATPase expression in the membrane fractions (1 μg) of K562-WT and K562-ABCG2 cells. (B) The relative densities of the bands were determined, and the densitometric ratios of ABCG2 to $Na^+/K^+$-ATPase were calculated. Cell viability after exposure to various (C) imatinib and (D) dasatinib concentrations in K562-WT (open circles) and K562-ABCG2 cells (closed circles) for 72 h. The cell viability after treatment with control (vehicle) was set at 100 %. Each data represents the mean ± S.E. (n = 3). Statistical analyses were performed using un-paired t-test. $*p < 0.05$ compared with that of K562-WT cells.

**Table 3**
The $IC_{50}$ values of imatinib and dasatinib in K562-WT and K562-ABCG2 cells after 72 h of exposure.

| Drugs | $IC_{50}$ (nM) | | *p* value |
|---|---|---|---|
| | K562-WT | K562-ABCG2 | |
| Imatinib | 152.8 ± 27.1 | 342.8 ± 72.6 | 0.013 |
| Dasatinib | 0.78 ± 0.11 | 1.74 ± 0.15 | 0.001 |

Each value represents the mean ± S.E. (n = 3). The $IC_{50}$ values of imatinib and dasatinib were calculated from the curves of cell viability in K562-WT and K562-ABCG2 cells (Fig. 2C and D). Statistical analyses were performed using the un-paired t-test. $IC_{50}$, 50 % inhibitory concentration.

another xanthine oxidase inhibitor, had no significant effects on the efficacy and residual concentration of dasatinib (Figs. 3A and 4). According to the package insert (Feburic® Tablet, Teijin Pharma Limited, Japan), in terms of the maximum febuxostat plasma concentration and blood cell transfer rate, the concentration of febuxostat in blood cells is estimated to be approximately 1.6–6.2 μM. In this study, the effect of 1–10 μM febuxostat in K562-ABCG2 cells was confirmed. Thus, these findings suggest that febuxostat enhances the efficacy of dasatinib at clinical concentrations by decreasing BCR::ABL1 phosphorylation via inhibition of ABCG2-mediated dasatinib efflux, rather than through xanthine oxidase inhibition. In addition, the effect of febuxostat was synergistic (Fig. 3B); hence, its combination with dasatinib therapy presents as a promising treatment strategy.

ABCG2 is expressed in various tissues, including the small intestine, liver, and kidney, and is responsible for the absorption, distribution, and excretion of ABCG2 substrates [16]. Miyata et al. [11] reported that febuxostat administration significantly increased plasma sulfasalazine (typical ABCG2 substrate) concentrations in mice. Thus, the inhibition of ABCG2-mediated dasatinib transport by febuxostat may increase plasma dasatinib concentrations, which may subsequently result in adverse events associated with dasatinib. However, this study demonstrated that there was no significant difference in the incidence of adverse events leading to dasatinib discontinuation between patients with and without febuxostat (Table 2). Thus, the side effects of concomitant febuxostat on dasatinib plasma concentrations is minimal. Given the small sample size in the present study, further investigation is necessary to confirm the altered pharmacokinetics of dasatinib and development of adverse events during co-administration with febuxostat.

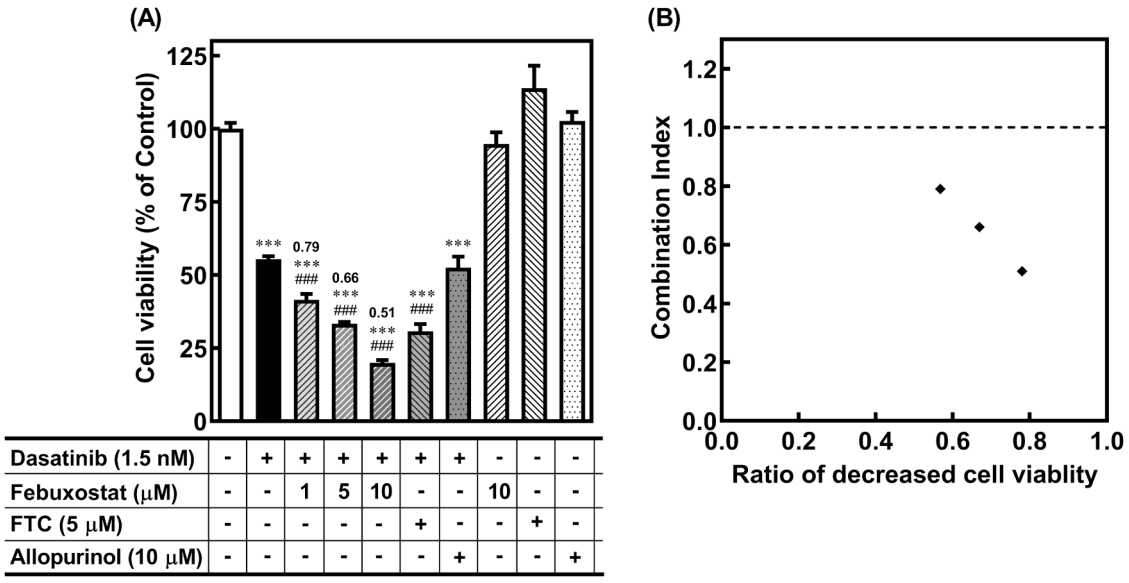


**Fig. 3.** Effect of febuxostat on K562-ABCG2 cell viability after dasatinib exposure. (A) K562-ABCG2 cells were incubated at 37°C for 72 h with vehicle (Control) or dasatinib (1.5 nM) in the absence or presence of febuxostat (1, 5, and 10 μM), FTC (typical ABCG2 inhibitor, 5 μM), or allopurinol (negative control, 10 μM). Cell viability after treatment with vehicle (control) was set at 100 %. Each column represents the mean ± S.E. (n = 6–9). $^{***}p < 0.001$ compared with that of the control. $^{###}p < 0.001$ compared with that of 1.5 nM dasatinib (+). Statistical analyses were performed using Tukey's multiple comparison test. (B) Effect (ratio of decreased cell viability)-combination index plot of febuxostat combination treatment. Combination index was calculated using the SynergyFinder. Combination index (CI) values for each combination are given above columns in (A). CI < 1, CI = 1, and CI > 1 denote synergism, additive activity, and antagonism, respectively. FTC, Fumitremorgin C.

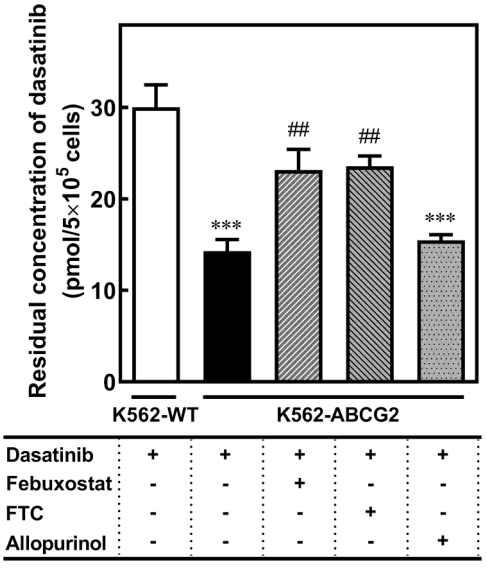


**Fig. 4.** Effect of febuxostat on residual dasatinib concentrations in K562-WT and K562-ABCG2 cells. The cells were incubated with incubation medium containing 10 μM dasatinib at 37°C for 30 min. After dasatinib was removed, the cells were pre-incubated with febuxostat (10 μM), FTC (typical ABCG2 inhibitor, 5 μM), or allopurinol (negative control, 10 μM) at 37°C. After pre-incubation for 30 min, dasatinib was effluxed from the cell by incubation in the presence of 4 mM ATP at 37°C for 5 min, and then the residual concentration of dasatinib was determined using LC-MS/MS. Each column represents the mean ± S.E. (n = 9). $^{***}p < 0.001$ compared with that of K562-WT cells. $^{##}p < 0.01$ compared with that of K562-ABCG2 cells without febuxostat, FTC, or allopurinol. Statistical analyses were performed using Tukey's multiple comparison test. FTC, Fumitremorgin C.

This study has some limitations that need to be considered. First, this clinical study included a small number of patients from a single institution; hence, the possibility of a selection bias should not be ruled out. Second, excluding the potential effects of other unknown confounders was difficult in this retrospective study. Third, the significant efficacy of dasatinib may have contributed to the development of tumor lysis syndrome, necessitating the use of febuxostat. In this study, febuxostat was administered before dasatinib therapy, indicating its use for the management of hyperuricemia rather than tumor lysis syndrome. However, the purpose of febuxostat use was not clear owing to the retrospective nature of this study. Fourth, it remains unclear whether febuxostat's inhibition of ABCG2-mediated dasatinib excretion from CML cells mainly contributes to the improvement of dasatinib efficacy in patients with CML. This is because information regarding the off-target effects of febuxostat and BCR::ABL1-dependent mechanisms, including BCR::ABL1 mutations, gene amplification, or upregulated expression, is limited and these may also contribute to the development of dasatinib resistance [4]. Finally, it is unclear where patients who did not achieve EMR and/or MMR have BCR::ABL1 mutation because data of BCR::ABL1 mutation was not obtained from electronic medical records. Moreover, Sokal and ELTS risk scores as prognostic indicators could not be evaluated because data of spleen size needed to calculate these scores was not available. Thus, future large-scale, multicenter prospective studies should be conducted to evaluate the effects of febuxostat on the safety, efficacy, and pharmacokinetics of dasatinib in patients with CML. Furthermore, *in vitro* and *in vivo* studies are required to elucidate the underlying mechanism by which febuxostat enhances the efficacy of dasatinib in patients with CML.

## 5. Conclusions

This study demonstrates for the first time that the concomitant use of febuxostat enhances the efficacy of dasatinib in patients with CML. This is at least, in part, by the inhibition of ABCG2-mediated dasatinib excretion from CML cells. Overall, these findings provide important insights for the improvement of CML treatment and overcoming TKI resistance.

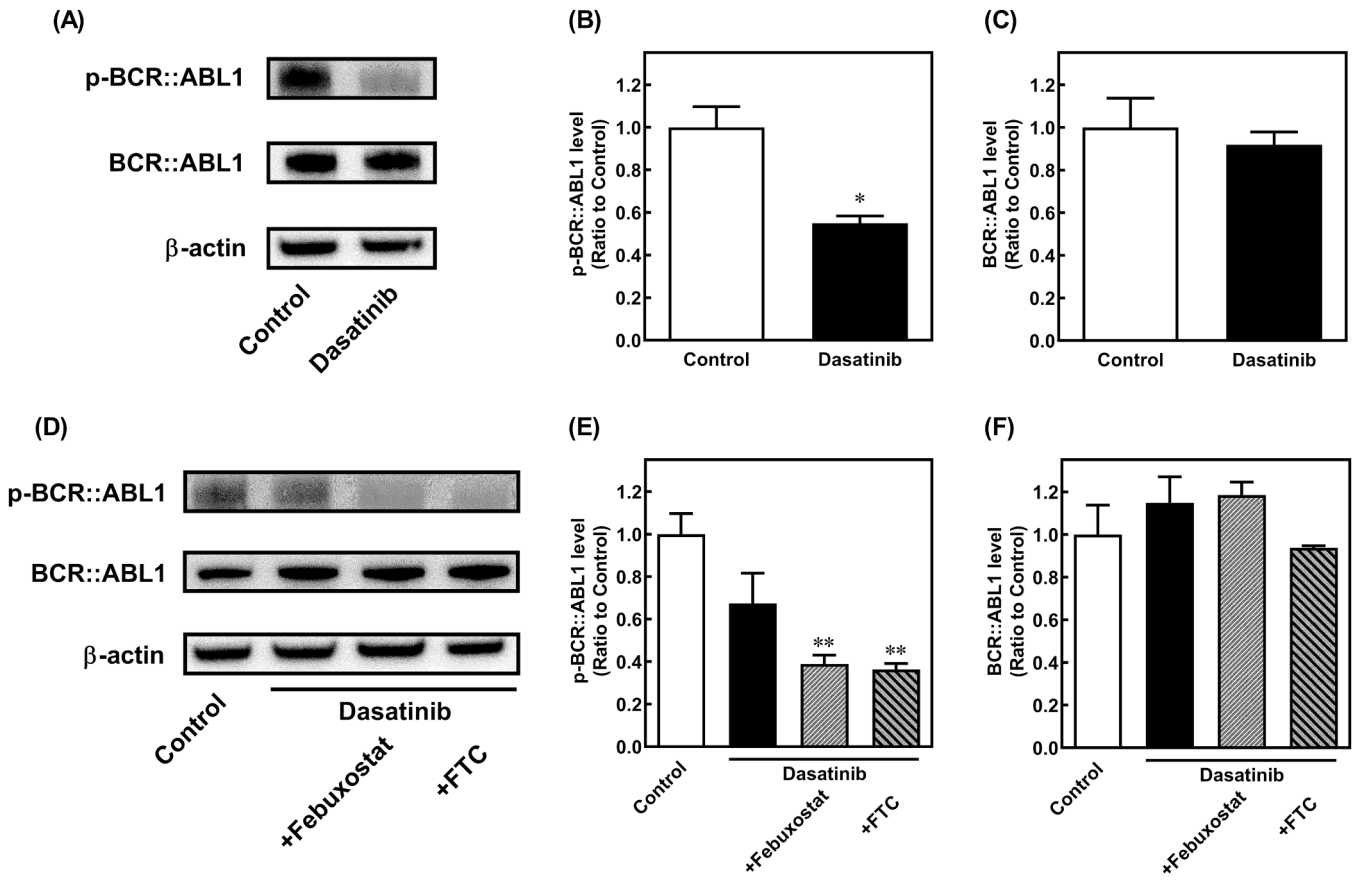


**Fig. 5.** Effect of febuxostat on BCR::ABL1 phosphorylation in K562-WT and K562-ABCG2 cells after dasatinib exposure. The cells were incubated at 37°C for 72 h with 1.5 nM dasatinib in the absence or presence of febuxostat (10 μM) or FTC (typical ABCG2 inhibitor, 5 μM) in (A, B, C) K562-WT and (D, E, F) K562-ABCG2 cells. Western blotting analysis was performed on total protein lysates (10 μg) for p-BCR::ABL1, BCR::ABL1, and β-actin. The relative band densities were determined, and the densitometric ratios of p-BCR::ABL1 or BCR::ABL1 to β-actin were calculated. Each column represents the mean ± S.E. (n = 3). Statistical analyses were performed using Dunnett's test. $^{*}p < 0.05$, $^{**}p < 0.01$, compared with that of the control (vehicle) in K562-WT and K562-ABCG2 cells. FTC, Fumitremorgin C.

## Funding

This work was supported by The Research Foundation for Pharmaceutical Science.

## CRediT authorship contribution statement

**Kenji Ikemura:** Writing – review & editing, Writing – original draft, Validation, Project administration, Methodology, Investigation, Funding acquisition, Formal analysis, Conceptualization. **Kotaro Kawashima:** Writing – original draft, Validation, Methodology, Investigation, Formal analysis. **Yuji Toyozumi:** Investigation. **Miho Takemura:** Investigation, Formal analysis. **Masahiro Okuda:** Writing – review & editing, Supervision, Conceptualization.

## Declaration of Competing Interest

The authors declare that they have no known competing financial interests or personal relationships that could have appeared to influence the work reported in this paper.

## Acknowledgements

We would like to thank Editage (www.editage.jp) for English language editing.

## References

[1] J.D. Rowley, Letter: a new consistent chromosomal abnormality in chronic myelogenous leukaemia identified by quinacrine fluorescence and Giemsa staining, Nature 243 (5405) (1973) 290–293.
[2] J.E. Cortes, G. Saglio, H.M. Kantarjian, M. Baccarani, J. Mayer, C. Boque, N. P. Shah, C. Chuah, L. Casanova, B. Bradley-Garelik, G. Manos, A. Hochhaus, Final 5-year study results of DASISION: the dasatinib versus imatinib study in treatment-naive chronic myeloid leukemia patients trial, J. Clin. Oncol. 34 (20) (2016) 2333–2340.
[3] S. Claudiani, F. Chughtai, A. Khan, C. Hayden, F. Fernando, J. Khorashad, V. Orovboni, G. Scandura, A. Innes, J.F. Apperley, D. Milojkovic, Long-term outcomes after upfront second-generation tyrosine kinase inhibitors for chronic myeloid leukemia: managing intolerance and resistance, Leukemia 38 (4) (2024) 796–802.
[4] J. Sun, R. Hu, M. Han, Y. Tan, M. Xie, S. Gao, J.F. Hu, Mechanisms underlying therapeutic resistance of tyrosine kinase inhibitors in chronic myeloid leukemia, Int. J. Biol. Sci. 20 (1) (2024) 175–181.
[5] Y. Toyoda, T. Takada, H. Suzuki, Inhibitors of human ABCG2: from technical background to recent updates with clinical implications, Front. Pharmacol. 10 (2019) 208.
[6] R.D. Cunha, S. Bae, D.J. Murry, G. An, TKI combination therapy: strategy to enhance dasatinib uptake by inhibiting Pgp- and BCRP-mediated efflux, Biopharm. Drug Dispos. 37 (7) (2016) 397–408.
[7] S. Shukla, Z.S. Chen, S.V. Ambudkar, Tyrosine kinase inhibitors as modulators of ABC transporter-mediated drug resistance, Drug Resist Updat 15 (1-2) (2012) 70–80.
[8] M. Delord, P. Rousselot, J.M. Cayuela, F. Sigaux, J. Guilhot, C. Preudhomme, F. Guilhot, P. Loiseau, E. Raffoux, D. Geromin, E. Genin, F. Calvo, H. Bruzzoni-Giovanelli, High imatinib dose overcomes insufficient response associated with ABCG2 haplotype in chronic myelogenous leukemia patients, Oncotarget 4 (10) (2013) 1582–1591.
[9] M. Spina, Z. Nagy, J.M. Ribera, M. Federico, I. Aurer, K. Jordan, G. Borsaru, A. S. Pristupa, A. Bosi, S. Grosicki, N.L. Glushko, D. Ristic, J. Jakucs, P. Montesinos, J. Mayer, E.M. Rego, S. Baldini, S. Scartoni, A. Capriati, C.A. Maggi, C. Simonelli, F. S. Group, FLORENCE: a randomized, double-blind, phase III pivotal study of

febuxostat versus allopurinol for the prevention of tumor lysis syndrome (TLS) in patients with hematologic malignancies at intermediate to high TLS risk, Ann. Oncol. 26 (10) (2015) 2155–2161.
[10] K. Ikemura, S.I. Hiramatsu, Y. Shinogi, Y. Nakatani, I. Tawara, T. Iwamoto, N. Katayama, M. Okuda, Concomitant febuxostat enhances methotrexate-induced hepatotoxicity by inhibiting breast cancer resistance protein, Sci. Rep. 9 (1) (2019) 20359.
[11] H. Miyata, T. Takada, Y. Toyoda, H. Matsuo, K. Ichida, H. Suzuki, Identification of febuxostat as a new strong ABCG2 inhibitor: potential applications and risks in clinical situations, Front. Pharmacol. 7 (2016) 518.
[12] F. Ito, M. Miura, Y. Fujioka, M. Abumiya, T. Kobayashi, S. Takahashi, T. Yoshioka, Y. Kameoka, N. Takahashi, The BCRP inhibitor febuxostat enhances the effect of nilotinib by regulation of intracellular concentration, Int. J. Hematol. 113 (1) (2021) 100–105.
[13] S. Zheng, W. Wang, J. Aldahdooh, A. Malyutina, T. Shadbahr, Z. Tanoli, A. Pessia, J. Tang, SynergyFinder Plus: toward better interpretation and annotation of drug combination screening datasets, Genom. Proteom. Bioinforma. 20 (3) (2022) 587–596.
[14] Y. Mukai, T. Yoshida, T. Kondo, N. Inotsume, T. Toda, Novel high-performance liquid chromatography-tandem mass spectrometry method for simultaneous quantification of BCR-ABL and Bruton's tyrosine kinase inhibitors and their three active metabolites in human plasma, J. Chromatogr. B Anal. Technol. Biomed. Life Sci. 1137 (2020) 121928.
[15] M. Kizaki, N. Takahashi, N. Iriyama, S. Okamoto, T. Ono, N. Usui, K. Inokuchi, C. Nakaseko, M. Kurokawa, M. Sumi, F. Nakamura, T. Kawaguchi, R. Suzuki, K. Yamamoto, K. Ohnishi, I. Matsumura, T. Naoe, Ti New, Efficacy and safety of tyrosine kinase inhibitors for newly diagnosed chronic-phase chronic myeloid leukemia over a 5-year period: results from the Japanese registry obtained by the New TARGET system, Int. J. Hematol. 109 (4) (2019) 426–439.
[16] D. Hira, T. Terada, BCRP/ABCG2 and high-alert medications: biochemical, pharmacokinetic, pharmacogenetic, and clinical implications, Biochem. Pharmacol. 147 (2018) 201–210.